

Electrical Properties of Segregated Ultrahigh Molecular Weight Polyethylene/Multiwalled Carbon Nanotube Composites

Ying Xi, Atsuko Yamanaka, Yuezhen Bin, Masaru Matsuo

Department of Textile and Apparel Science, Faculty of Human Life and Environment, Nara Women's University, Nara 630-8263, Japan

Received 28 November 2006; accepted 3 January 2007

DOI 10.1002/app.26282

Published online 16 May 2007 in Wiley InterScience (www.interscience.wiley.com).

ABSTRACT: Multiwalled carbon nanotubes (MWNTs) and ultrahigh molecular weight polyethylene (UHMWPE) composites are prepared using paraffin as solvent. The resulting electrical properties show lower electrical percolation threshold, which is 1.4 vol %, than that of UHMWPE-MWNT composites prepared by gelation/crystallization from decalin solution. Good reproducibility and higher maximum of electrical conductivity are obtained. The extremely low electrical percolation threshold indicates that the dispersion of MWNTs is segregated, which can be proved by the morphology of the film observed by optical

microscopy. The complex planes of electric modulus are useful to analyze the dispersion of MWNTs and the quality of interparticle contacts. In addition, the result of thermogravimetry shows that the retardation of onset of UHMWPE decomposition in inert gas is observed in the mixture with MWNTs. © 2007 Wiley Periodicals, Inc. *J Appl Polym Sci* 105: 2868–2876, 2007

Key words: multiwalled carbon nanotubes; ultrahigh molecular weight polyethylene; electrical properties; electrical percolation threshold; heat decomposition

INTRODUCTION

Conductive polymer composites (CPCs) are obtained by adding conductive fillers like carbon black (CB), graphite (G), carbon fibers (CFs), or metal particles to polymer matrix. CPCs exhibit several interesting features due to their good electrical conductivity, light weight, corrosion resistance, and reinforced mechanical properties. Examples of application that used CPCs include battery and fuel cell electrodes, as well as antistatic and corrosion-resistant materials. Common conductive fillers are CB, G, and CF. These composites are characterized by a percolation threshold or a critical value at which the conductivity starts to increase as a function of filler contents. However, the mechanical properties decrease seriously at high filler contents (>15 wt %, usually). Therefore, much attention has been centered on the preparation of conducting composites with a low percolation threshold. Researches on carbon nanotubes (CNTs) have increased significantly over the past decade, because of their extraordinary physical properties, such as the electrical and thermal properties, the axial elastic modulus. With the development of CNTs, many recent researches have been done on the CPCs with CNTs as

conductivity fillers to achieve a low percolation threshold concentration and high electrical conductivity.^{1,2} Zhang et al.² developed a new method to prepare composites, spraying CNTs suspended solution onto the surface of polymer powders. And then the composites can be processed by melt processing method after water is vaporized. The low percolation threshold was achieved by this method. For ultrahigh molecular weight polyethylene (UHMWPE), its high melting viscosity, unfortunately, limits the use of the melt processing method. The gelation/crystallization from solution has been proven to be more effective than the other methods to disperse carbon fillers in the UHMWPE matrix. In our previous research,³ the high oriented polyethylene composites filled with aligned CNTs in place of CB were prepared successfully by gelation/crystallization from solution, which leads to a lower percolation threshold and higher maximum conductivity. Furthermore, the dispersion of multiwalled carbon nanotubes (MWNTs) could be improved drastically using small amount of ethylene-methyl methacrylate copolymer as one of components, when MWNTs with curved grapheme sheets with few defects were used as fillers into UHMWPE matrix.⁴

In this article, using the paraffin as solvent, the segregated UHMWPE-MWNT composites were made. Compared with our previous results,^{3,4} the lower percolation threshold and higher maximum conductivity are obtained because the new method using the paraf-

Correspondence to: M. Matsuo (m-matsuo@cc.nara-wu.ac.jp).

fin as solvent can disperse MWNTs as isolated agglomerates in the matrix rather than a network of the particles.

EXPERIMENTAL

UHMWPE (Hizex; Mitsui Chemicals) with an average viscosity molecular weight ($\bar{M}_v = 6,300,000$) and fibrous type MWNTs were used as test specimen. MWNTs used in our experiment are Hyperion Graphite Fibrils with the diameter (D) of 10–20 nm, and the aspect ratio (L/D) of 1 to 2×10^3 . The BET surface area is 250 m²/g, and the DBP adsorption is 400–500 cm³/100 g. The true density is 2.0 g/cm³.

Figure 1 shows the scanning electron microscope (SEM) image and the Raman spectrum at excitation laser wavelength of 488 nm. Figure 1(a) indicates the MWNTs possess high purity and uniform diameter distribution. In Raman spectrum of Figure 1(b), however, the peak of the Raman-allowed phonon mode, E_{2g} , at about 1582 cm⁻¹ is not very sharp, and the intensity of the peak at 1345 cm⁻¹ is high, which appears through the disorder-induced phonon mode due to the infinite size of crystals and defects. It indicates the present MWNTs have a low degree of graphitization, and then they could be dispersed uniformly into UHMWPE matrix without admixing EMMA.

To make UHMWPE-MWNT composites, MWNTs were first stirred with UHMWPE in paraffin solvent at room temperature for 48 h and the mixture became a black glossy paste. And then the mixture was kept stirring and heated with a mild heating rate about 10°C/min up to 250°C and maintained for 30 min under nitrogen gas. The concentration of UHMWPE was decided to be 5 g against 20 g paraffin. This was the optimum concentration of UHMWPE to make MWNTs well distributed in solution and to form a uniform film later. The hot homogenized mixture was moved to a glass beaker with benzene solvent at room temperature. The benzene solvent was used to remove paraffin from the composites.

After paraffin was removed, the mixture was pressed between aluminum flat plates with mirror finished surfaces under a pressure of 2 MPa at 180°C for 20 min, and then was cooled slowly to room temperature. The prepared sheets were about 1.2 mm thick. In this method, the solvent quantity was very low compared with the gelation method. Therefore, the crystal lamellae of UHMWPE could not unfold fully due to its high viscosity and the dispersion of MWNTs was mainly in the amorphous region of UHMWPE.

Electrical conductivity at room temperature and electrical conductivity against temperature from 40 to 160°C at the 5°C/min heating rate were measured by high resistance measuring device (HR-100) produced by Iwamoto Seisakusho. The digital multimeter was

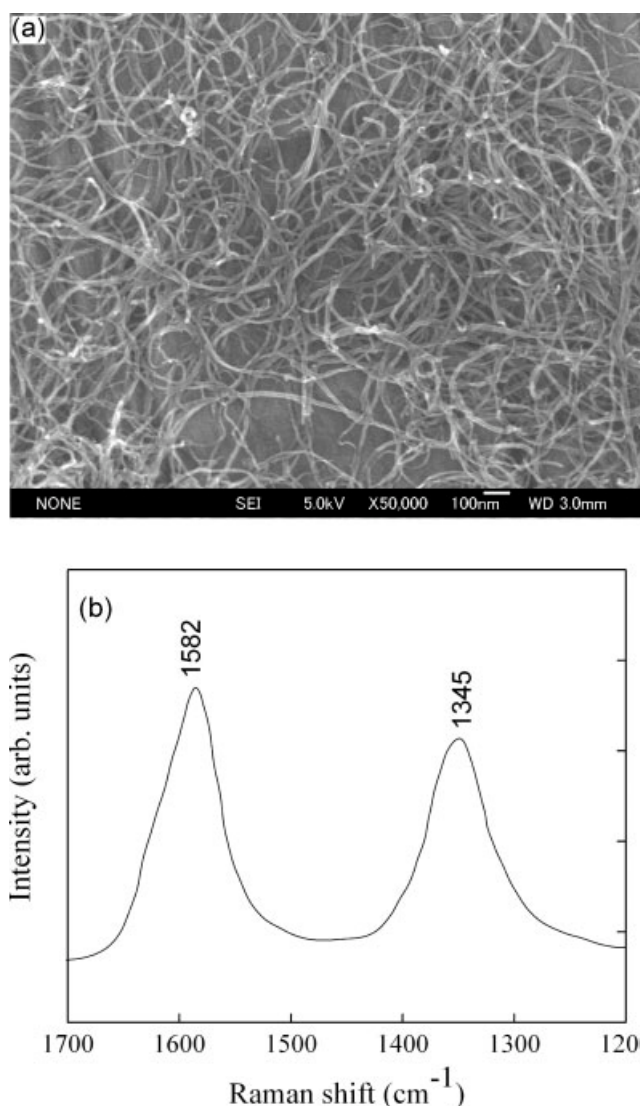


Figure 1 (a) SEM image and (b) Raman spectrum of original MWNTs.

used (Advantest R6441A Digital Multimeter) when the resistivity was lower than $10^7 \Omega \text{ cm}$. On the other hand, the measurements were done using a high resistance meter (HP 4339B High Resistivity Meter) when the resistivity exceeded beyond $10^7 \Omega \text{ cm}$. The results were presented as a logarithm of electrical conductivity ($\log(\text{S/cm})$). The dielectric property investigation was performed at temperature in the range of 10^2 – 10^6 Hz using a Solartron Impedance/Gain phase Analyzer 126096W model. Thermogravimetric analysis (TGA) measurement was done using TG/DTA 6300 (SII NanoTechnology); the sample was heated under N₂ from room temperature to 800°C at a heating rate of 10°C/min.

RESULTS AND DISCUSSION

Figure 2(a) shows the electric conductivity as a function of the conductive filler content in the UHMWPE-

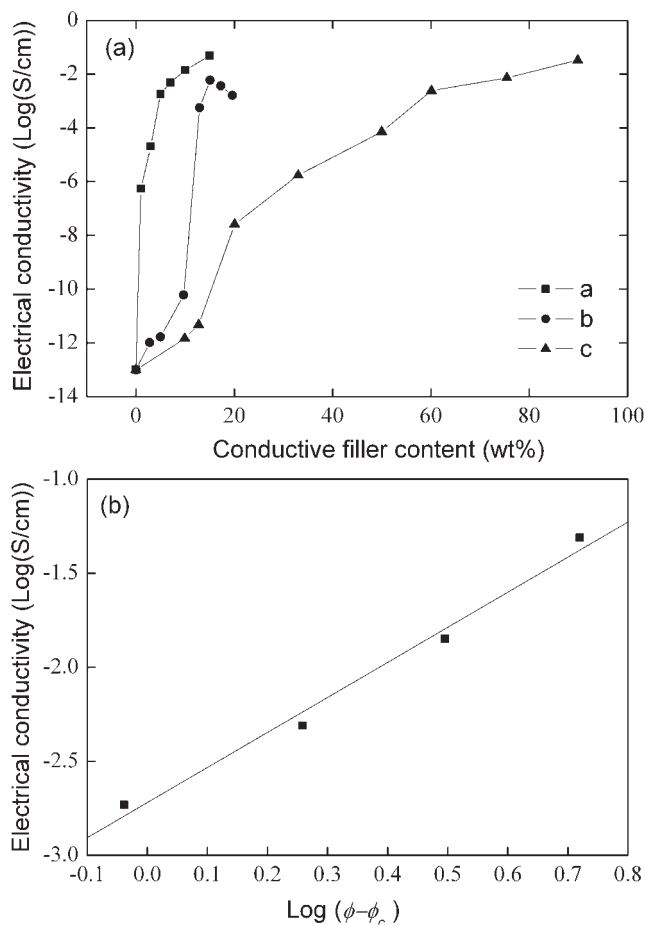


Figure 2 (a) Electrical conductivity as a function of conductive filler content: a, UHMWPE-MWNT composites prepared using paraffin as solvent; b, UHMWPE-MWNT composites prepared by the gelation/crystallization from decalin solution; c, UHMWPE-CB composites prepared by the gelation/crystallization from decalin solution. (b) Log-log plot of the conductivity against $\phi - \phi_c$ with $\phi_c = 1.4$ vol % according to Eq. (1). Straight line was plotted by least-square method and has a slope $t = 1.86$.

based composites measured at room temperature. To compare the percolation threshold of composites, the electric conductivity of both UHMWPE-CB composites and UHMWPE-MWNT composites prepared by the gelation/crystallization from decalin solution is shown concurrently here.^{3,5}

It is shown that the percolation threshold of the UHMWPE-MWNT composites prepared by using paraffin as solvent, which is about 3 wt % (the volume content is about 1.4 vol %), is much lower than that of the UHMWPE-CB composites prepared by the gelation/crystallization from decalin solution, and also lower than UHMWPE-MWNT composites prepared by the gelation/crystallization from decalin solution. This low percolation threshold is a direct consequence of the segregated distribution, which leads to the formation of long conductive network of the

conductive filler already at such very low content (Fig. 3).

Percolation theory predicts the relationship between the composite conductivity and volume content of the conductive filler as

$$\sigma = \sigma_0(\phi - \phi_c)^{-t} \quad \text{for } \phi > \phi_c \quad (1)$$

where σ_0 is a constant, ϕ is the volume content of the filler, ϕ_c is the critical volume content at percolation threshold, which is 1.4 vol % in the present article. The critical exponent of percolation conductivity t generally reflects the dimensionality of the system with values theoretically around 1 and 2 for two and three-dimensions, respectively. However, t value was given to be about 3 experimentally for the composite filled with randomly oriented fibers,⁶ and about 1.36 experimentally for the composite filled with multi-wall nanotubes.⁷ For the present composites, t value was determined to be 1.86 from the slope of the straight line shown in Figure 2(b), which is similar to that reported by Kilbride et al.⁷

The morphology of the composites is studied by optical microscopy. The sample thickness for optical microscopy is about 3 μm . Figure 3 shows that the distribution of MWNTs in UHMWPE is segregated. The similar morphology can also be found in UHMWPE-CB composites.⁸ The transparency region is the crystalline region of UHMWPE. MWNTs are mainly dispersed in amorphous region and the gaps between crystals because lamella construction of crystalline regions does not permit the migration of MWNTs to them.

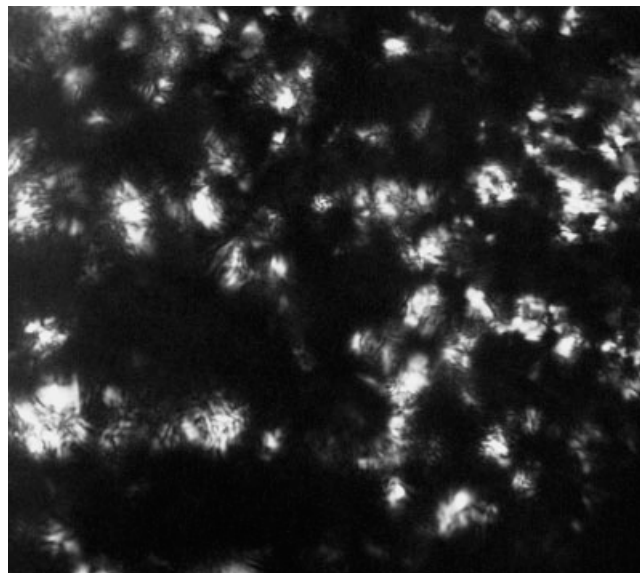


Figure 3 Morphology of 5% UHMWPE-MWNT composite observed by optical microscopy ($\times 40$).

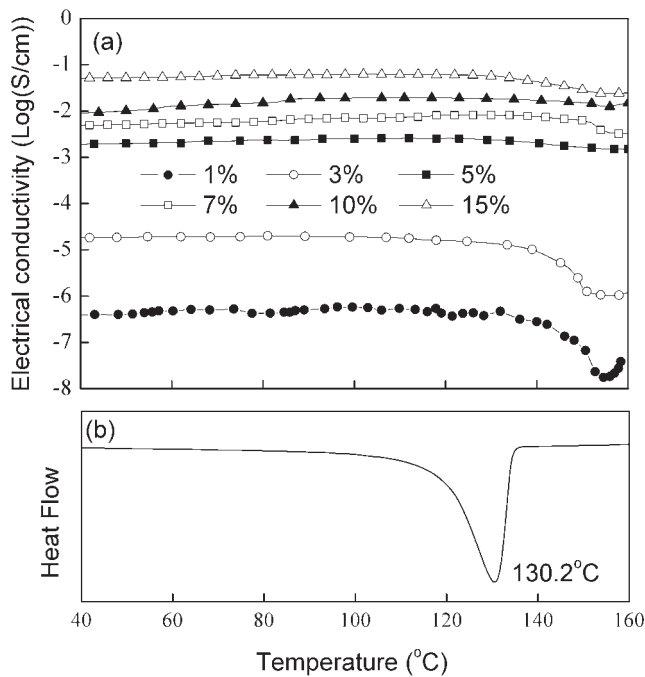


Figure 4 (a) Electrical conductivity as a function of temperature of the composites with different MWNT content; (b) the DSC curve of pure UHMWPE.

For the composites of semicrystalline polymer and conductive fillers, especially polyethylene and carbon particles (CBs or CFs), the positive temperature coefficient (PTC) effect caused by melting of the matrix crystallites have been reported.^{3,5,9} Figure 4 shows the electrical conductivity of the UHMWPE-MWNT composites as a function of temperature with different MWNT content and the DSC curve of pure UHMWPE. The results indicate that the PTC effect also happen at the temperature above the melting point of UHMWPE, and the intensity of PTC effect, which is R_p/R_{RT} defined as the ratio of peak resistivity R_p to the room temperature resistivity R_{RT} , is dependent on the MWNT content. At MWNT high content, the composites behave more or less like a zero-temperature-coefficient material. As the MWNT content decreases, the intensity of PTC effect increases. Compared with that of the composites of polyethylene and CB⁴ or CFs,⁹ the intensity of PTC effect of UHMWPE-MWNT composites is not so large considering the higher agglomerating force and bigger aspect ratio of MWNTs. Moreover, the thermal expansion of UHMWPE beyond the melting point is not significant enough to cause the separation of the contacted MWNTs, especially when the MWNT content is high, so the conductive paths for charge transportation still exist.

As is well known, the thermoplastic conductive composites exhibit poor reproducibility of electrical conductivity–temperature curves for different heating/cooling runs, which is obviously due to the fact

that the expansion/contraction processes accompanying heating/cooling cycles cause movements of the fillers and the behaviors is irreversible. By introducing UHMWPE into the matrix, the reproducibility of electrical conductivity provided good satisfaction, since the high viscosity of UHMWPE minimizes the migration of the conductive fillers and the deformation even in the temperature range beyond the melting point. Actually, the same tendency was confirmed for the admixture of small amount of UHMWPE such as the system LMWPE-UHMWPE (90/10)-CF.⁹ Figure 5 shows the electric conductivity measured against temperature for UHMWPE-MWNT films with 15 wt % of MWNTs under three runs. From Figure 5, the good reproducibility of electrical conductivity–temperature curves can be observed even at the highest MWNT content.

Figure 6(a) shows the dependence of dielectric constant on frequency of UHMWPE-MWNT composites with different MWNT contents. It is well known that the pure polyethylene is nonpolar polymer, so it has no dielectric dissipation and a low dielectric constant, practically independent of frequency and temperature. As the MWNT content increases, a pronounced dependence of dielectric constant on frequency is observed. This is a direct consequence of the interfacial relaxation between the UHMWPE matrix and MWNTs.

Above the percolation threshold (3% MWNT content), a step can be observed clearly, which is shifted to higher frequency when increasing MWNT content in polymer matrix. The dependence of dielectric constant on the frequency can be given by

$$\epsilon' \propto \frac{f_0^2}{f^2 + f_0^2} \quad (2)$$

Equation (2) is a stepwise function, where the critical frequency f_0 is the temperature-dependent parameter, which increases with the increasing temperature.

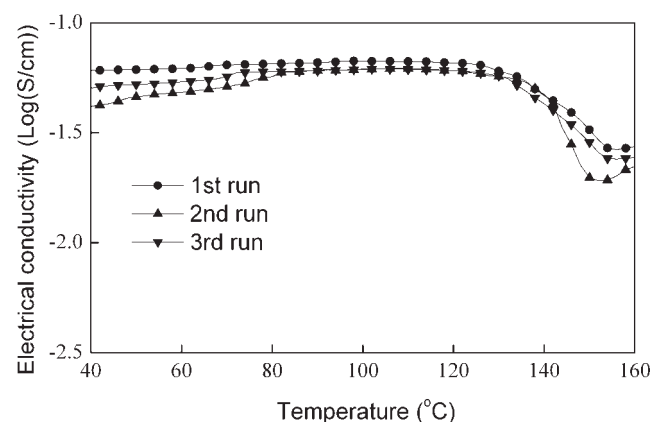


Figure 5 Electrical conductivity as a function of temperature of UHMWPE-MWNT composites with 15 wt % MWNT under three runs.

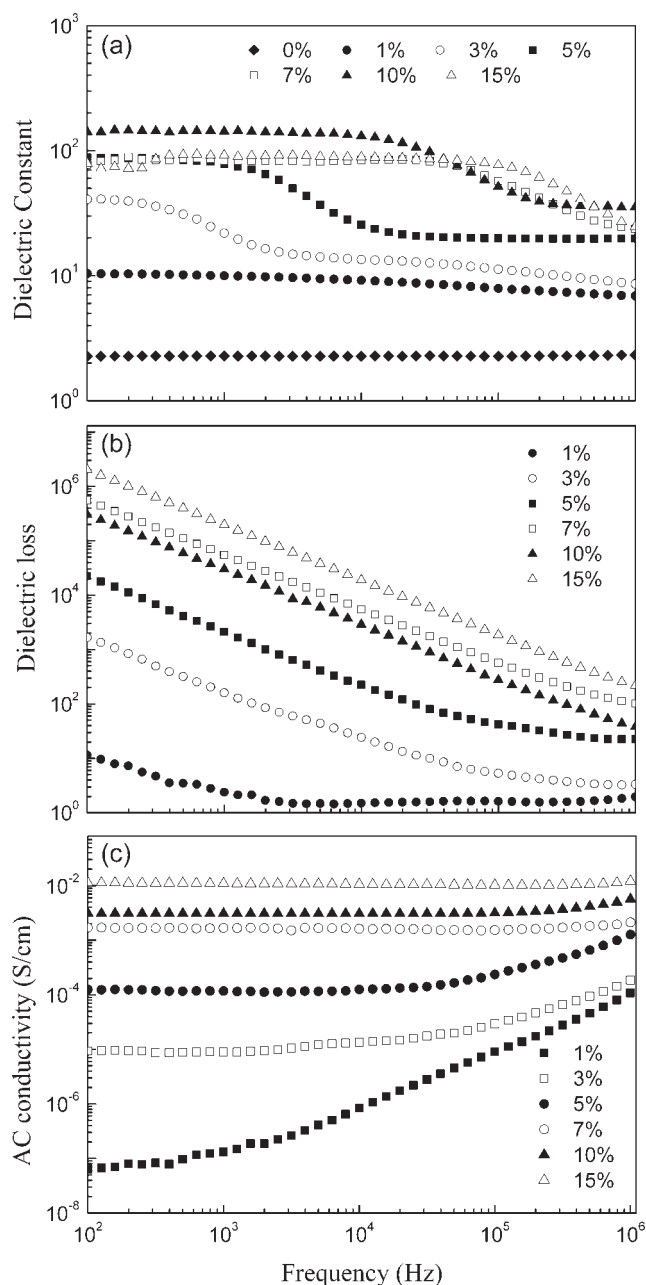


Figure 6 (a) Dielectric constant, (b) dielectric loss, and (c) AC conductivity as a function of frequency for UHMWPE-MWNT composites with different MWNT content.

At the lower frequency ($f \ll f_0$), ϵ' is independent on the frequency. At higher frequency ($f \gg f_0$), ϵ' is decreased with the increasing frequency.

Figure 6(b) shows the dependence of dielectric loss on frequency of UHMWPE-MWNT composites with different MWNT content. When MWNT content is above 7%, the plots of dielectric loss are the straight line and the slope of these lines is about -1 , which means that DC conductivity is more significant than interfacial polarization at higher MWNT content. When MWNT content is below 7% and the frequency is higher than 10^4 Hz, the plots of dielectric loss

change from straight lines to sigmoidal curves. These sigmoidal curves indicate that the interfacial polarization becomes pronounced since the interfacial polarization equation of dielectric loss does not follow a linear behavior at higher frequencies.¹⁰ At the same time, because no relaxation peaks appear in the plots of dielectric loss although these peaks were predicted by the step of the dielectric constant in Figure 6(a).

Figure 6(c) shows the dependence of AC electric conductivity on the frequency of UHMWPE-MWNT composites with different MWNT content. At low MWNT content (1%), the conductivity increases with frequency, following the power law $\sigma(f) \sim f^s$ where s is the critical exponent, which follows the inequality $0 \leq s \leq 1$, characterizing hopping conduction. For 3–5% MWNT content, the conductivity remains nearly independent of the frequency below 10^4 Hz, and at higher frequency, the conductivity increases with frequency following the power law $\sigma(f) \sim f^s$ just like 1% MWNT content. When increasing the MWNT content above 7%, the conductivity becomes less dependent on the frequency and the frequency value of the step shifts to higher frequency. The DC conductivity plateaus, which appear above 7% MWNT content, mean that the AC conductivity is similar to the conductivity measured by DC method. This DC conductivity plateaus further prove that DC conductivity is more significant than interfacial polarization at higher MWNT content, which was discussed in Figure 6(b). We may conclude that an infinite cluster is present when the content is higher than the percolation threshold.

Figure 7 represents the variation of dielectric constant as a function of MWNT content at the fixed frequency ($f = 10^3$ Hz). It is worth noting that the

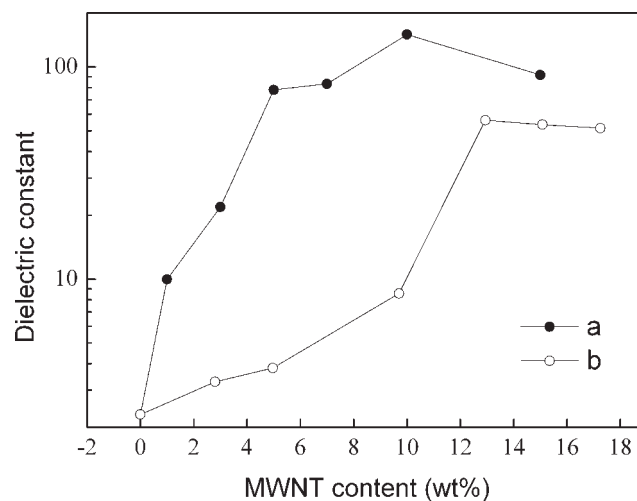


Figure 7 Dielectric constant as a function of MWNT content at the fixed frequency ($f = 10^3$ Hz). (a) UHMWPE-MWNT composites prepared using paraffin as solvent; (b) UHMWPE-MWNT composites prepared by the gelation/crystallization from decalin solution.

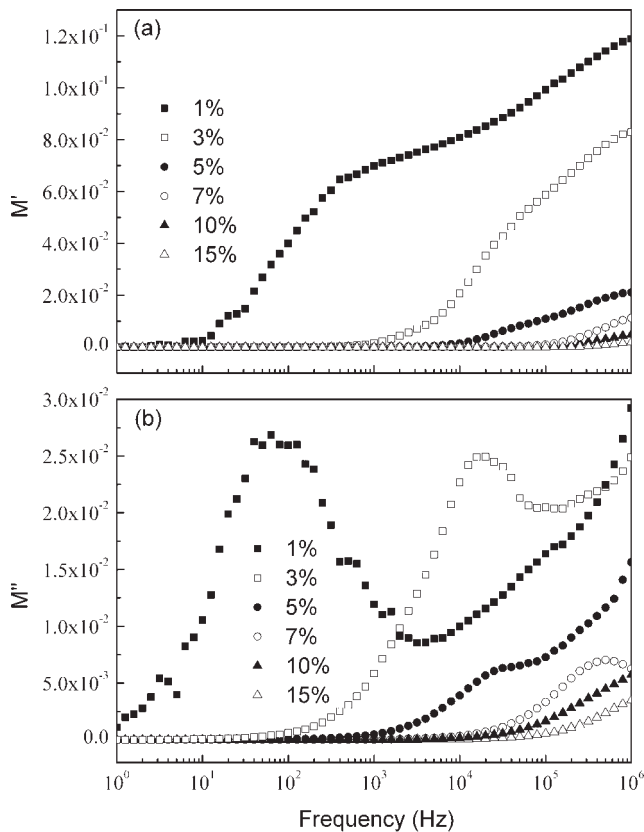


Figure 8 The electric modulus as a function of frequency with different MWNT content: (a) the real part and (b) the imaginary part.

dielectric constants of UHMWPE-MWNT composites, whether prepared using paraffin as solvent or by the gelation/crystallization from decalin solution, increase sharply at the percolation threshold like the conductivity of composite. The dielectric constant increases moderately above the percolation threshold, and decreases a little at higher MWNT content due to high conductivity. This is due to the fact that a network of MWNT particles is gradually formed within the matrix with the increasing MWNT content, thereby leading to an increase in dielectric constant. And heterogeneous dispersion of fillers in the polymer matrix is another crucial factor affecting the dielectric behavior. More heterogeneous the dispersion is, the dielectric constant is larger. Accordingly, the dispersion of MWNT particles in UHMWPE-MWNT composites prepared using paraffin as solvent is more heterogeneous than that of UHMWPE-MWNT composites prepared by the gelation/crystallization from decalin solution, since the dielectric constant of the former is larger than that of the latter.

In addition, the experimental data is also analyzed using the formalism of electric modulus, which is introduced by McCrum et al.¹¹ and also is used to study the conductivity relaxation behaviors of polymer.¹² An advantage of adopting the electric modulus to interpret

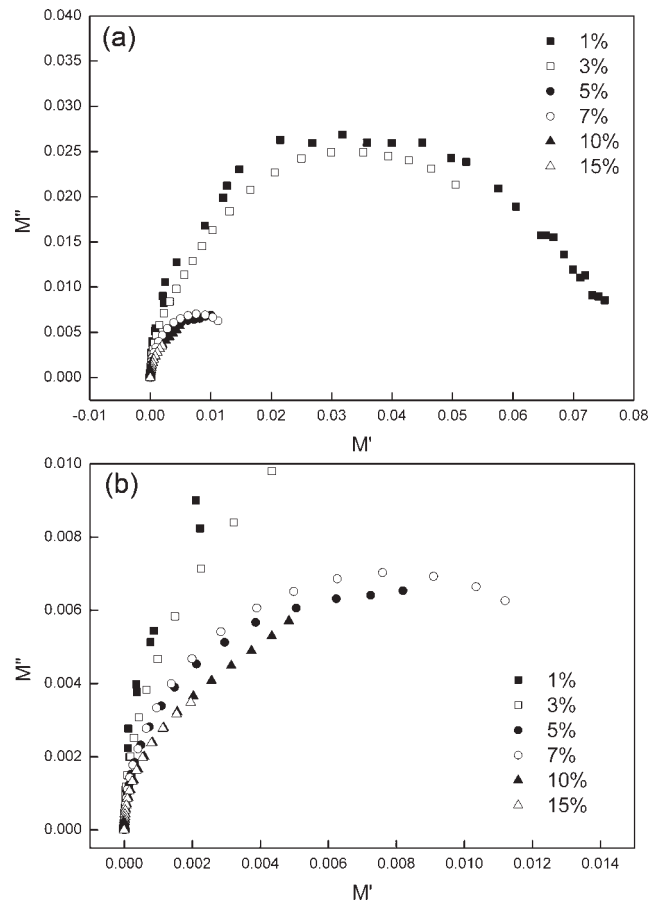


Figure 9 (a) Complex planes for the electric modulus at different MWNT contents; (b) the magnification of (a).

bulk relaxation properties is that variations in the large values of permittivity and conductivity at low frequencies are minimized. In this way the familiar difficulties caused by electrode nature and contact, space charge injection phenomena, and absorbed impurity conduction effects can be resolved or ignored.¹³

Complex modulus M^* , which is the inverse complex permittivity, is defined by the following equation:

$$M^* = \frac{1}{\epsilon^*} = \frac{1}{\epsilon' - i\epsilon''} = \frac{\epsilon'}{\epsilon'^2 + \epsilon''^2} + i \frac{\epsilon''}{\epsilon'^2 + \epsilon''^2} = M' + iM'' \quad (3)$$

where M' and M'' are the real and the imaginary electric modulus, and ϵ' and ϵ'' are the real and the imaginary permittivity, respectively.

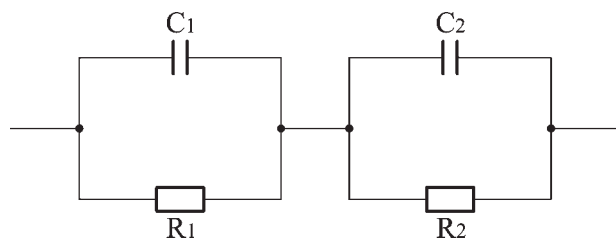


Figure 10 The equivalent circuit used to simulate the data of UHMWPE-MWNT composites.

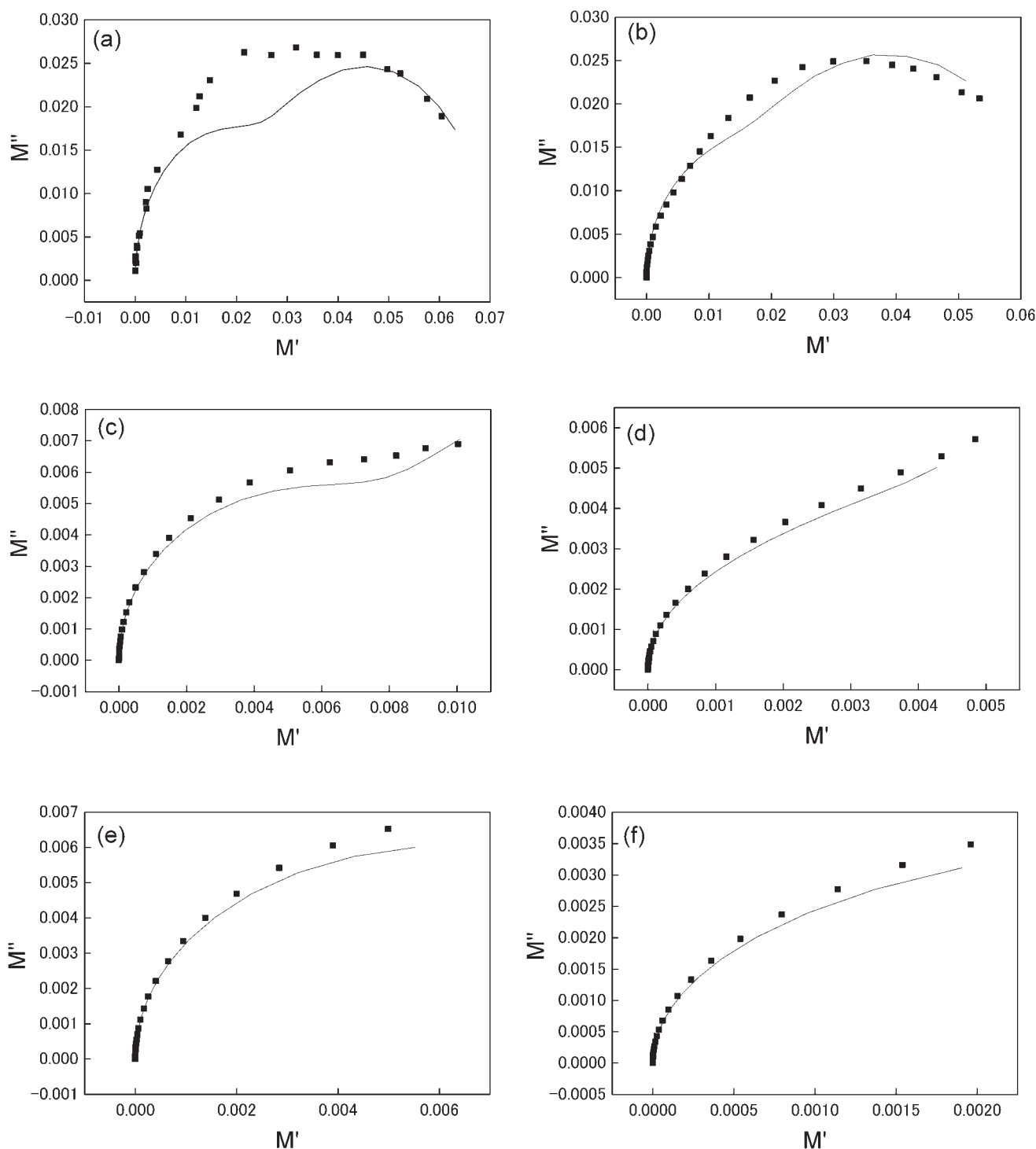


Figure 11 Complex planes for the electric modulus at different MWNT contents: (a) 1%; (b) 3%; (c) 5%; (d) 7%; (e) 10%; (f) 15%; lines are the results calculated by the equivalent circuit.

The real and image part of electric modulus M' and M'' as a function of frequency with different MWNT content is shown in Figure 8. The loss peaks of M'' , which is obscured by conductivity in the plots of ϵ'' , can be observed. Therefore, this is evident that imaginary part of the electric modulus is more suitable than the dielectric loss for the polymer composites with high electrical conductivity.

The complex planes for the electric modulus at different MWNT contents are shown in Figure 9. At the lower MWNT content (below 3%), the semicircle with large radii can be observed, which indicates that MWNTs in the matrix do not form the conductive network very well. While with the MWNT content increasing, the shape of the curves changes from the semicircles to the arcs, and the radii becomes smaller gradually.

On the basis of the MWNT dispersion, which consists of the two regions with poor contacts and good contacts of MWNT, respectively, the equivalent circuit for these two kinds of dispersion of MWNT may be depicted by a parallel combination of C_1 and R_1 in series with a parallel arrangement of C_2 and R_2 , as shown in Figure 10. R_1 , C_1 elements refer to the resistance and the capacitance of the region with poor contacts of MWNTs. And the R_2 , C_2 elements refer to the resistance and the capacitance of the region with good contacts of MWNTs. Accordingly, the complex impedance of the equivalent network can be obtained as follows:

$$Z = \frac{1}{i\omega C_1 + \frac{1}{R_1}} + \frac{1}{i\omega C_2 + \frac{1}{R_2}} \quad (4)$$

The two RC parallel elements in series describe two semicircles in the complex planes for electric modulus. One semicircle in the higher frequency, refer to the R_1 , C_1 parallel elements, indicates the region with poor contacts of MWNTs, and the other semicircle in the lower frequency, refer to the R_2 , C_2 parallel elements, indicates the region with good contacts of MWNTs. The results of the simulation are shown in Figure 11. The corresponding parameters are listed in Table I. The calculated line is in good agreement with the experimental data except for the composite with 1% MWNT content.

As listed in Table I, both R_1 and R_2 decreased with the increasing MWNT content, and the gap between them decreased. At the same time, the C_1 and C_2 increased. The changes of the two RC parallel elements indicate that the contacts of MWNT become better when the MWNT content is increased. In the complex plane of for electric modulus, the corresponding semicircle referring to the region with poor contacts of MWNTs will gradually disappear with increasing MWNT content, which is in agreement with the experimental complex planes of electric modulus very well.

After discussing electrical properties of UHMWPE-MWNT composites, we must emphasize that the stabilization effect of MWNTs on pyrolytic decomposi-

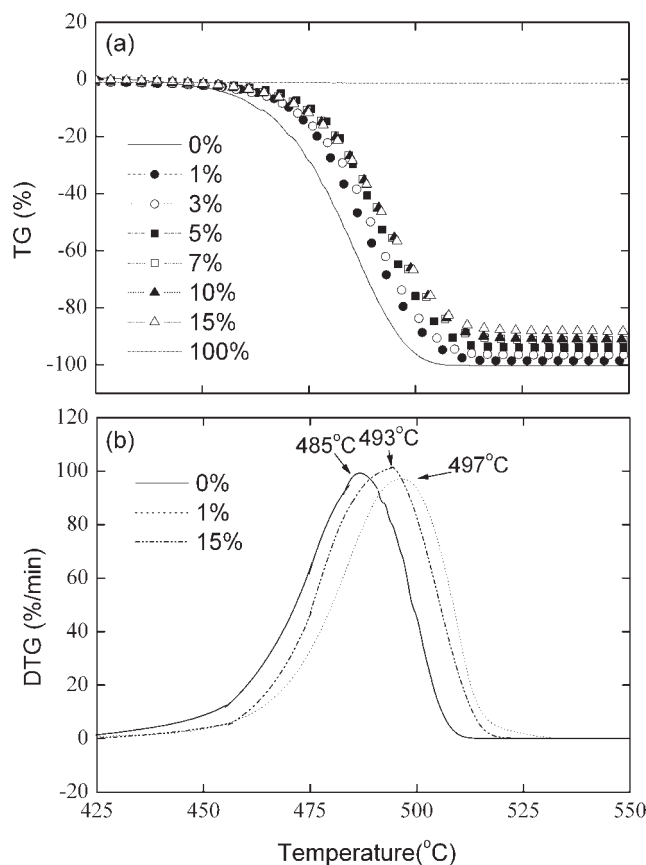


Figure 12 (a) TG of UHMWPE, MWNT, and composites, in a nitrogen atmosphere; (b) DTG of UHMWPE and composites, in a nitrogen atmosphere.

tion of UHMWPE. The TGA is performed on composites from 0 to 100% concentration, and it is carried out under a nitrogen atmosphere, which minimized the mass loss of MWNT oxidation, and allowing UHMWPE to thermally decompose completely and the char yield is about zero at the same time. The resulting curves are shown in Figure 12(a). The masses remaining at 520°C are almost due to the remaining MWNTs, and are consistent with the initial MWNT loading.

Comparison of the curves in Figure 12(b), the peak of DTG curve shifts to about 8°C higher temperature in the blend with 1% MWNT content and shifts to about 12°C higher temperature by increasing MWNT content to 15%. It reveals that there is a retardation of the onset of UHMWPE decomposition for the composites even with low MWNT loadings at about 1%, and also there is an effect on the start and the end of the degradation, which shifts to the higher temperature for the samples with MWNTs.

As is well known, polyethylene decomposes by random scission, producing homologous series of n -alkenes, n -alkanes, and n -alkadienes. The retardation of UHMWPE decomposition mentioned earlier is

TABLE I
Parameters Evaluated for the Equivalent Network

MWNT content (wt %)	R_1 (Ω)	C_1 (pF)	R_2 (Ω)	C_2 (pF)
1	8×10^7	27	9×10^5	23
3	8×10^5	29	5×10^4	21
5	7×10^4	91	6×10^3	39
7	5×10^3	140	9×10^2	55
10	2×10^3	150	6×10^2	90
15	7×10^2	160	1×10^2	93

likely to be a result of absorption, by the activated carbon surface, of free-radicals generated during polymer decomposition. At higher temperatures or loading the decomposition of the oxidized nanotube surface itself negates the stabilizing effect. Other researchers had also reported that MWNTs can stabilize some polymers,^{14–16} and they consider the stabilization effect of MWNTs is probably similar to that of carbon families such as fullerene (C₆₀) and CB. Therefore, the activated carbon surface gives rise to less chain scissions and the retardation of the radical chain reactions as confirmed by the decreased rate of decomposition and the higher decomposition temperature. At the same time, MWNTs do not affect the qualitative results of PE pyrolysis since MWNTs are just a retarder of UHMWPE decomposition.

CONCLUSIONS

Different from the traditional gelation/crystallization from decalin solution that used in making UHMWPE gel and its composites, the segregated UHMWPE-MWNT composites have been made using the paraffin as solvent. The resulting electrical properties show lower electrical percolation threshold and good reproducibility of electrical conductivity. The dielectric spectroscopy is done for the characterization of the state dispersion of MWNTs in polymer matrix. The dielectric constant has a sharp increase at the percolation threshold like the conductivity of composite. The extremely low electrical percolation threshold indicates that the dispersion of MWNTs is segregated, which also can be proved by the optical microscopy observation. The electric modulus formalism is considered suitable for the investigation of the polymeric

composites with a conductive component. The complex planes of electric modulus are used to analyze the dispersion of MWNTs and the quality of interparticle contacts. In addition, the retardation of onset of UHMWPE decomposition in inert gas is observed in the mixture with MWNTs, judging by TG and DTG curves of UHMWPE shifting to higher temperature.

References

1. Sandler, J. K. W.; Kirk, J. E.; Kinloch, I. A.; Shaffer, M. S. P.; Windle, A. H. *Polymer* 2003, 44, 5893.
2. Zhang, Q.; Rastogi, S.; Chen, D.; Lippits, D.; Lemstra, P. J. *Carbon* 2006, 44, 778.
3. Bin, Y.; Kitanaka, M.; Zhu, D.; Matsuo, M. *Macromolecules* 2003, 36, 6213.
4. Chen, Q.; Bin, Y.; Matsuo, M. *Macromolecules* 2006, 39, 6528.
5. Xu, C.; Agari, Y.; Matsuo, M. *Polym J* 1998, 30, 372.
6. Sternstein, S.; Zhu, A. J. *Macromolecules* 2002, 35, 7262.
7. Kilbride, B. E.; Coleman, J. N.; Fraysse, J.; Fournet, P.; Cadek, M.; Drury, A.; Hutzler, S.; Roth, S.; Blau, W. J. *J Appl Phys* 2002, 92, 4024.
8. Chan, C. M.; Cheng, C. L.; Yuen, M. M. F. *Polym Eng Sci* 1997, 37, 1127.
9. Xi, Y.; Ishikawa, H.; Bin, Y.; Matsuo, M. *Carbon* 2004, 42, 1699.
10. Bluma, G. S.; Maria, E. L.; Guilherme, M. O. B.; Dipak, K. *Eur Polym J* 2006, 42, 676.
11. MécCrum, N. G.; Read, B. E.; Williams, G. *Anelastic and Dielectric Effects in Polymeric Solids*; Wiley: New York, 1967.
12. Macedo, P. B.; Moynihan, C. T.; Bose, R. *Phys Chem Glasses* 1972, 13, 171.
13. Tsangaris, G. M.; Psarras, G. C.; Kouloumbi, N. *J Mater Sci* 2027 1998, 33.
14. Jin, Z. X.; Pramoda, K. P.; Xu, G. Q.; Goh, S. H. *Chem Phys Lett* 2001, 337, 43.
15. Zou, Y. B.; Feng, Y. C.; Wang, L.; Liu, X. B. *Carbon* 2004, 42, 271.
16. Jakab, E.; Blazsó, M. *J Anal Appl Pyrol* 2002, 64, 263.